Modern NIR Spectrometer Technology for Real-Time State-of-Charge Estimation of Heat Storage Materials

Evgeny Legotin[1,2(✉)], Gayaneh Issayan[3], Bernhard Zettl[3], Markus Brandstetter[1], and Christian Rankl[1]

[1] RECENDT – Research Center for Non-Destructive Testing GmbH, Science Park 2, Altenberger Straße 69, 4040 Linz, Austria
evgeny.legotin@recendt.at

[2] TU Wien, Institute of Chemical, Environmental and Bioscience Engineering, Getreidemarkt 9, 1060 Vienna, Austria

[3] Energy Research Group ASIC, University of Applied Sciences Upper Austria, Stelzhamerstraße 23, 4600 Wels, Austria

Abstract. Sorption heat storage is expected to play an important role in future thermal energy systems, particularly in buildings and industrial processes. For optimal operation, it is important to control the parameters of heat storage systems, such as the state-of-charge. In this study, we show the possibility to use compact and cost-effective micro-opto-electro-mechanical spectroscopic sensors for state-of-charge control of diverse sorption heat storage materials.

Keywords: heat storage · silica gel · zeolite · salt-hydrate composite · near-infrared spectroscopy · micro-spectrometer

1 Introduction

Global energy challenges urge the development of new energy storage solutions. A diversified, renewable, and decentralized energy supply is critical to ensure the future energy security. An optimized balancing of energy flows between energy producers and consumers should reduce possible losses and increase the resilience of energy networks.

Thermal energy storage systems are well-suited to store geothermal and solar energy, both for seasonal and daily demands. The three main types of thermal energy storage are sensible, latent, and thermochemical heat storage, the latter being based on either chemical reactions or sorption processes. In recent years, increasingly more attention has been paid to sorption heat energy storage. In comparison to sensible and latent heat storages, thermochemical heat storage is notable for high energy densities, robustness, low heat losses, and good cycling stability [1, 2].

Some important characteristics of sorption heat storage materials are adsorption capacity, cyclability, state-of-health (SOH) as well as state-of-charge (SOC) which in case of sorption heat storage refers to the relative amount of sorbate (e.g. water) taken up

P. Schossig et al. (Eds.): IRES 2022, AHE 16, pp. 288–296, 2023.
https://doi.org/10.2991/978-94-6463-156-2_19

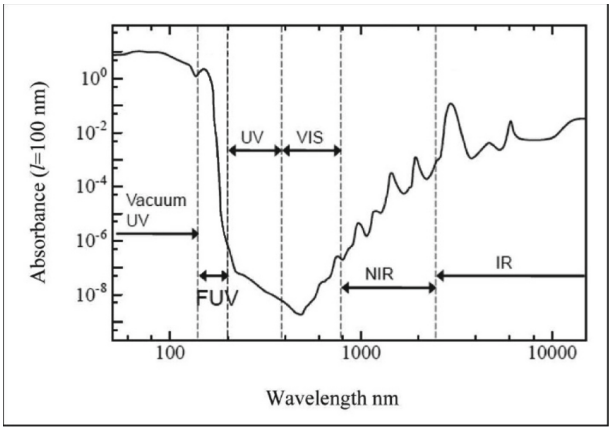

Fig. 1. The absorption spectrum of water with different wavelength regions shown (adapted from [7]).

by the sorbent. A suitable technology to control these parameters in real-time is required to ensure the efficient operation.

To the best of our knowledge, no specific sensors to estimate the real-time SOC of sorption heat storage systems are available on the market today. Recently, a capacitive SOC sensor prototype has been developed, which employs the relative change of material permittivity during water sorption and desorption processes [3]. Another promising approach is the use of infrared spectroscopic sensors to estimate the amount of sorbate adsorbed by the storage material.

Infrared spectroscopy allows identification and quantification of substances in a contactless and non-destructive way, based on their characteristic absorption bands. Enabled by the specific absorption bands of water located in the infrared region (Fig. 1), the method is generally suitable for quantitative determination of water adsorbed by solids. Examples are known from pharmaceutical [4], food [5], textile [6], and other industries. Recent advances such as the development of micro-opto-electro-mechanical (MOEMS) devices enable a cost-effective IR spectroscopic process analytics [8, 9].

Earlier, the feasibility of SOC prediction using near-infrared (NIR) MOEMS technology was demonstrated in lab scale on a zeolite material [10]. In the present study, we demonstrate the use of the MOEMS-based NIR spectrometer technology for real-time SOC estimation of various sorption heat storage materials, including microporous silica gel, zeolites as well as in-house prepared salt-hydrate composites.

2 Materials and Methods

2.1 Materials

Silica gel beads for this study were purchased from OKER-CHEMIE GmbH (Germany). Zeolite materials were acquired from CWK Chemiewerk Bad Köstritz GmbH (Germany). Three different zeolite materials were investigated, viz. Two A-type zeolites

Table 1. Essential material properties according to the material datasheets [12]–[15] (if applicable). A hyphen (-) denotes no data available.

Material type	Trade name or designation	Chemical composition	Bead / granule size, mm	Pore size, Å	Water vapor adsorption capacity, wt%
A-type zeolite (LTA)	KÖSTROLITH® 4AK	$Na_2O{\cdot}Al_2O_3{\cdot}2SiO_2{\cdot}nH_2O$ (+ binder)	1.6–2.5	4	≥ 21.5 (20 °C, 55% RH)
A-type zeolite (LTA), binder-free	KÖSTROLITH® 4ABFK	$Na_2O{\cdot}Al_2O_3{\cdot}2SiO_2{\cdot}nH_2O$	2.5–5.0	4	≥ 24.0 (20 °C, 55% RH)
NaY-type zeolite (FAU), binder-free	KÖSTROLITH® NaYBFK	$Na_2O{\cdot}Al_2O_3{\cdot}mSiO_2{\cdot}nH_2O$ (m ~ 5)	1.6–2.5	9	≥ 29 (20 °C, 55% RH)
Silica gel	SIOGEL® microporous, white, beads	$SiO_2{\cdot}nH_2O$	2.5–4.0	-	≥ 10.0 (23 °C, 20% RH) ≥ 21.5 (23 °C, 40% RH) ≥ 31.0 (23 °C, 80% RH)
Salt-hydrate composite	Salt-hydrate composite A	Clinoptilolite: 75 wt% $CaCl_2{\cdot}2H_2O$ + $LiCl{\cdot}H_2O$: 20 wt% (mixing ratio 7:1) Portland cement: 5 wt%	> 4	-	-
Salt-hydrate composite	Salt-hydrate composite B	Clinoptilolite + birch fibers: 40 wt% $CaCl_2{\cdot}2H_2O$ + $LiCl{\cdot}H_2O$: 40 wt% (mixing ratio 9:1) Buzzi Unicem Next base CSA cement: 20 wt%	~ 7 (in diameter)	-	-

(binder-containing and binder-free) and a binder-free NaY-type zeolite. Salt-hydrate composites were prepared by the granulation method as described in [11]. In this study, they are designated as salt-hydrate composite A and salt-hydrate composite B. Figure 2 shows the appearance of the materials under study, while chemical compositions and physical characteristics are summarized in Table 1.

Prior to each measurement, the samples were charged in a drying chamber (FED 115, BINDER, Germany), then cooled down to the room temperature in a desiccator. Silica gel and zeolite samples were dried for 3 h at 150 °C and 250 °C, respectively. Salt-hydrate composite samples was dried for 2 h at 100 °C, then for another 2 h at 200 °C.

2.2 Data Acquisition

Water sorption measurements of the charged heat storage materials were carried out on a lab-scale set-up that enables a probeless and non-invasive acquisition of NIR spectra in diffuse reflection geometry (Fig. 3).

Fig. 2. Tested thermal energy storage materials: a) A-type zeolite; b) A-type zeolite binder-free; c) NaY-type zeolite binder-free; d) silica gel; e) salt-hydrate composite A; f) salt-hydrate composite B.

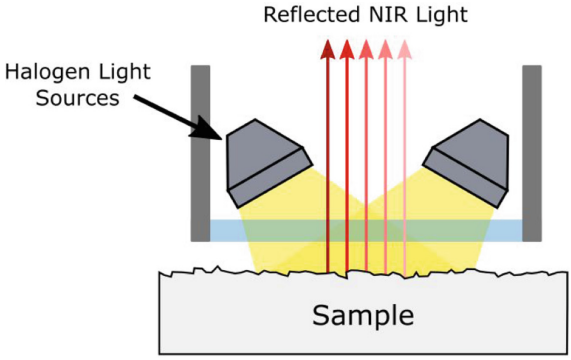

Fig. 3. Schematic image explaining the principle of a NIR measurement in diffuse reflection geometry.

NIR spectroscopic measurements were performed in the spectral range of 1750–2150 nm with a step of 5 nm using a NIR Fabry–Pérot micro-spectrometer with integrated light sources (NIRONE 2.2, Spectral Engines, Finland). Sheet aluminium served as the reference standard.

Changes in sample mass were recorded using an analytical balance (CP224S-0CE, Sartorius, Germany) having a precision of 0.1 mg. The initial sample mass (in the charged state) was in the range of 16–28 g, which depends on the material.

All measurements were conducted in ambient conditions. A typical experiment duration was 5–6 days. Spectral and gravimetric data were collected every 120 s.

2.3 Data *Preprocessing* and *Chemometric Modelling*

As the signals acquired by the spectrometer module and by the balance were not synchronized, an interpolation of the sample mass readings was performed (method: cubic spline). Before the interpolation, gravimetric data were smoothed (adjacent-averaging filter, 5 points window, polynomial order: 2).

Partial least squares (PLS) regression models were developed using the OriginPro 2021b software package. The full spectrum dataset was used for modelling. The absorbances at each wavelength served as the independent variables and the relative mass change (in % to the initial mass of the sample after drying) was used as the dependent variable. The maximum number of factors was set to 10. The root mean square error of cross-validation (RMSECV) as well as the R-squared (R^2) were calculated in the traditional way.

3 Results and Discussion

Although water has several absorption bands in the NIR spectral region (Fig. 1), the absorption band at about 5150 cm^{-1} ($\lambda \approx 1940$ nm), representing a combination of asymmetric stretching and bending vibrations of water molecules, is particularly suitable for quantification of adsorbed water in various materials [16, 17]. Based on this, a spectral range of 1750–2150 nm was chosen for the measurements, which covers the aforementioned absorption band of water.

Figure 4 visualizes the absorption NIR spectra of the studied materials as 2D contour plots where absorbance is plotted in colour scale. The respective gravimetric curves are presented at the top of each plot.

Water uptake occurs fast at the beginning but gradually slows down until saturation is achieved when the mass change curve reaches a plateau. Slight fluctuations in the mass of the samples could be caused by daily changes in the ambient air temperature and humidity. The achieved maximum water uptake values of commercial materials (zeolites, silica gel) are in good agreement with the water adsorption capacities specified in the material datasheets (Table 1). Among the commercial materials, the highest water vapor adsorption capacity was achieved for the binder-free NaY-type zeolite, followed by the binder-free and the binder-containing A-type zeolites. The in-house prepared salt-hydrate composite A exhibits a good storage stability as well as a high water vapor adsorption capacity comparable to those of the zeolite materials. The maximum mass change achieved for this material under the conditions of the experiment was 24% which suggests a water content of at least 19 wt% in the discharged material.

The obtained predicted vs. reference plots for water uptake are presented in Fig. 5. In most cases, the use of 6 latent variables was necessary for a satisfactory PLS model. The achieved R-squared exhibit values of at least 0.9955, while RMSECV values were all below 0.01. The analysis shows a satisfactory prediction of the amount of the adsorbed water.

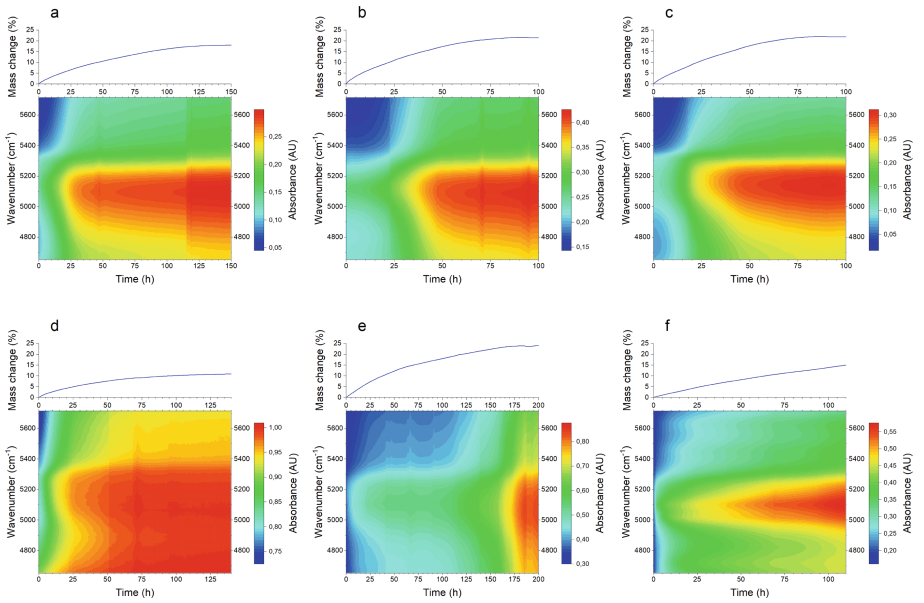

Fig. 4. NIR spectra and gravimetric curves of the studied heat storage materials: a) A-type zeolite; b) A-type zeolite, binder-free; c) NaY-type zeolite, binder-free; d) silica gel; e) salt-hydrate composite A; f) salt-hydrate composite B.

In case of the salt-hydrate composite B, we observed a slight swelling of the granulate due to water uptake. Because there was a concern that the granulate can come in contact with the spectrometer, which would affect the analytical balance readings, the experiment was interrupted. Swelling inevitably leads to a change in the optical path length of infrared light and can have an unfavourable effect on the measurement accuracy. Using a different optical interface and a different experimental set-up (e.g. in-tank measurement) would supposedly allow that the optical path length changes can be neglected.

It is to mention that no desorption measurements were conducted as part of this study as the latter was rather designed for fast screening. Lab-scale sorption and desorption in-tank measurements under controllable conditions are ongoing.

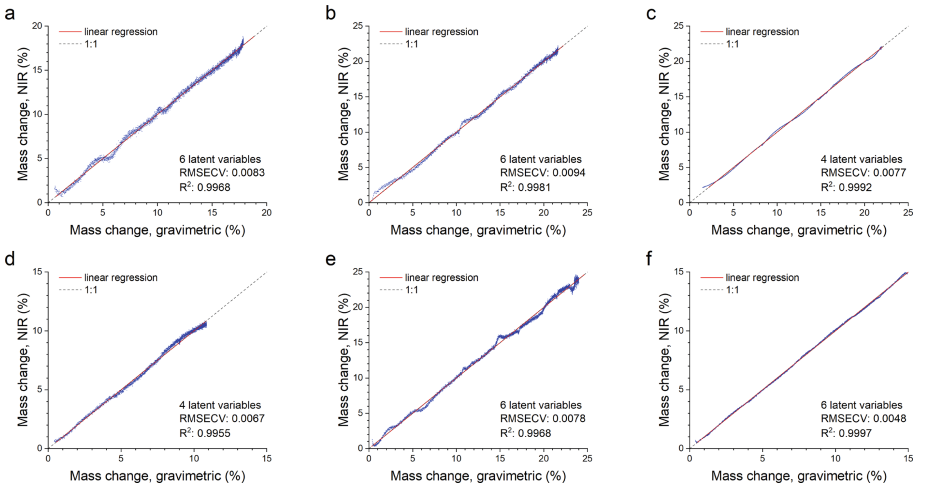

Fig. 5. Predicted vs. reference plots for the studied heat storage materials: a) A-type zeolite; b) A-type zeolite, binder-free; c) NaY-type zeolite, binder-free; d) silica gel; e) salt-hydrate composite A; f) salt-hydrate composite B.

4 Conclusion

In this work we showed that novel MOEMS-based NIR spectrometers can provide an adequately precise, compact, and low-cost solution for SOC control of heat storage systems. Based on the water adsorption measurement, we developed PLS models that show high accuracy of water content prediction. Presented research findings will help to assess heat storage capacities, improve balancing local heat supplies and demands, and therefore, increase the resilience of future heat distribution networks.

Acknowledgments. The authors acknowledge the European Regional Development Fund and the government of Upper Austria for financial support in the framework of the IWB2020 program. We are beholden to Verena Karl and Ivan Alic from RECENDT for technical assistance and component development work, respectively.

Authors' Contributions. G.I. and B.Z. prepared the salt-hydrate composites. E.L. conducted the measurements, the PLS modelling, and wrote the manuscript. B.Z., M.B., and C.R. contributed to scientific discussions and reviewed the manuscript.

Abbreviations

CSA	Calcium sulfoaluminate
FAU	Faujasite-type zeolite
LTA	Linde type-A zeolite

MOEMS	Micro-Opto-Electro-Mechanical Systems
NIR	Near-infrared
PLS	Partial least squares
RH	Relative humidity
RMSECV	Root mean square error of cross validation
SOC	State-of-charge
SOH	State-of-health

References

1. K.E. N'Tsoukpoe, H. Liu, N. Le Pierrès, L. Luo, A Review on Long-Term Sorption Solar Energy Storage, Renewable and Sustainable Energy Reviews 13(9) (2009) 2385–96. https://doi.org/10.1016/j.rser.2009.05.008
2. J. Zhang, H. Cho, P.J. Mago, Energy conversion systems and Energy storage systems, in: D. Borge-Diez, E. Rosales-Asensio (Eds.), Energy Services Fundamentals and Financing, Academic Press, 2021, pp. 155–179. https://doi.org/10.1016/B978-0-12-820592-1.00007-5
3. H. Kirchsteiger, A Novel State of Charge Sensor Concept for Thermochemical Heat Storage, in: Proceedings of the ISES EuroSun 2020 – 13th International Conference on Solar Energy for Buildings and Industry, 2020. https://doi.org/10.18086/eurosun.2020.07.09
4. C.R. Avila, J. Ferré, R.R. de Oliveira, A. de Juan, W.E. Sinclair, F.M. Mahdi, A. Hassanpour, T.N. Hunter, R.A. Bourne, F.L. Muller, Process Monitoring of Moisture Content and Mass Transfer Rate in a Fluidised Bed with a Low Cost Inline MEMS NIR Sensor, Pharmaceutical Research 37: 84 (2020). https://doi.org/10.1007/s11095-020-02787-y
5. A. Malvandi, H. Feng, M. Kamruzzaman, Application of NIR Spectroscopy and multivariate analysis for non-destructive evaluation of apple moisture content during ultrasonic drying, Spectrochimica Acta Part A: Molecular and Biomolecular Spectroscopy 269 (2022). https://doi.org/10.1016/j.saa.2021.120733
6. O. Daikos, T. Scherzer, Monitoring of the residual moisture content in finished textiles during converting by NIR hyperspectral imaging, Talanta 221 (2021). https://doi.org/10.1016/j.talanta.2020.121567
7. Y. Ozaki, Y. Morisawa, A. Ikehata, N. Higashi, Far-Ultraviolet Spectroscopy in the Solid and Liquid States: A Review, Applied Spectroscopy 66(1) (2012) 1–25. https://doi.org/10.1366/11-06496
8. R. Zimmerleiter, J. Kager, R. Nikzad-Langerodi, V. Berezhinskiy, F. Westad, C. Herwig, M. Brandstetter, Probeless non-invasive near-infrared spectroscopic bioprocess monitoring using microspectrometer technology, Analytical and Bioanalytical Chemistry 412 (2019) 2103–2109. https://doi.org/10.1007/s00216-019-02227-w
9. R. Zimmerleiter, E. Leiss-Holzinger, E.M. Wagner, K. Kober-Rychli, M. Wagner, M. Brandstetter, Inline biofilm monitoring based on near-Infrared spectroscopy with ultracompact spectrometer technology, NIR news 31(7-8) (2020) 9–13. https://doi.org/10.1177/0960336020978716
10. P. Luoma, P. Müller, H. Kirchsteiger, P. Kefer, M. Brandstetter, Feasibility of Next Generation Infrared Microspectrometers Demonstrated on Characterization of Zeolite Materials, 4th European Conference on Process Analytics and Control Technology (EuroPACT2017), Potsdam, Germany, 2017.

11. G. Issayan, B. Zettl, W. Somitsch, Developing and Stabilizing Salt-Hydrate Composites as Thermal Storage Materials, in: Proceedings of the 14th International Renewable Energy Storage Conference 2020 (IRES 2020), 2021, pp. 49–57. https://doi.org/10.2991/ahe.k.210202.008
12. CWK Chemiewerk Bad Köstritz GmbH (Germany), Product information, KÖSTROLITH® 4AK, Jul. 2014, provided by manufacturer
13. CWK Chemiewerk Bad Köstritz GmbH (Germany), Product information, KÖSTROLITH® 4ABFK, Jan. 2013, provided by manufacturer
14. CWK Chemiewerk Bad Köstritz GmbH (Germany), Product information, KÖSTROLITH® NaYBFK, Jan. 2013, provided by manufacturer
15. OKER-CHEMIE GmbH (Germany), Product information, PI-No.: SIO-02, Nov. 2021 [Revision: 09]
16. A.A. Chirsty, P. Sivarukshy, Comparison of adsorption properties of commercial silica and rice husk ash (RHA) silica: A study by NIR spectroscopy, Open Chemistry 19(1) (2021) 426–431. https://doi.org/10.1515/chem-2021-0044
17. M. Manley, Near-infrared spectroscopy and hyperspectral imaging: non-destructive analysis of biological materials, Chemical Society Reviews 43(24) (2014) 8200–8214. https://doi.org/10.1039/c4cs00062e